Time delay and Doppler estimation for wideband acoustic signals in multipath environments

Xue Jiang
Department of Electrical and Computer Engineering, McMaster University, Hamilton, Ontario, L8S 4K1, Canada

Wen-Jun Zeng[a)]
Department of Information Science and Electronic Engineering, Zhejiang University, Hangzhou 310027, China

Xi-Lin Li
Department of Computer Science and Electrical Engineering, University of Maryland Baltimore County, Baltimore, Maryland 21250

(Received 5 January 2011; revised 17 June 2011; accepted 17 June 2011)

Estimation of the parameters of a multipath underwater acoustic channel is of great interest for a variety of applications. This paper proposes a high-resolution method for jointly estimating the multipath time delays, Doppler scales, and attenuation amplitudes of a time-varying acoustical channel. The proposed method formulates the estimation of channel parameters into a sparse representation problem. With the ℓ_1-norm as the measure of sparsity, the proposed method makes use of the basis pursuit (BP) criterion to find the sparse solution. The ill-conditioning can be effectively reduced by the ℓ_1-norm regularization. Unlike many existing methods that are only applicable to narrowband signals, the proposed method can handle both narrowband and wideband signals. Simulation results are provided to verify the performance and effectiveness of the proposed algorithm, indicating that it has a super-resolution in both delay and Doppler domain, and it is robust to noise.
 [DOI: 10.1121/1.3609118]

PACS number(s): 43.60.Pt, 43.60.Jn, 43.60.Dh [WMC] Pages: 850–857

I. INTRODUCTION

Multipath propagation often arises in such fields as sonar, underwater acoustic communications, geoacoustic inversion, and acoustic source localization.[1–4] In a multipath environment, due to multiple reflections or scattering from the boundaries, the received signal can be represented as the superposition of a number of time-delayed and amplitude-attenuated versions of the original transmitted waveform. In addition, if any of the reflecting boundaries have a nonzero radial velocity component relative to the receiver, a Doppler effect will be imposed on the corresponding received multipath component. In this case, the multipath channel exhibits time variation, and the Doppler effect should be taken into account. In the narrowband case where the signal bandwidth is much smaller than the carrier frequency, the Doppler effect can be well approximated by a *Doppler frequency shift*.[5] However, acoustic signals are often wideband. Hence the narrowband assumption is invalid, and the Doppler effect should be described by *Doppler scale*.[5–7] The Doppler scale results in compression or dilation of the received signal in time-scale. Knapp and Carter pointed out that the effect of time compression (or expansion) should be taken into account in this case.[8] However, the signal model in Ref. 8 is based on single direct path propagation and does not consider the multipath.

In many applications, it is of interest to estimate the parameters of multipath components, including time delays, amplitudes, and Doppler scales, and remove the multipath effects. Several techniques, e.g., the least squares,[9] the Gibbs sampling,[10] and the ℓ_1-norm deconvolution,[4] have been proposed to estimate the multipath channel parameters when there are no Doppler effects. When the Doppler effects are considered, the channel response to be estimated is a function defined on the two-dimensional (2D) delay-Doppler plane. The basic approach to estimate the 2D delay-Doppler function is the matched filtering, which includes computing the cross-ambiguity function of the transmitted and received signals.[7] The major drawback of the matched filtering is that its resolution is limited to the width of the main lobe of the ambiguity function. To improve the delay-Doppler resolution, the inverse filtering based deconvolution approach was proposed.[5] However, this approach[5] can only handle narrowband signals and is not applicable to the wideband case. Habboosh *et al* developed an algorithm for detecting closely spaced delay/Doppler components that can be used for wideband signals.[6] This algorithm reduces the ill-conditioning by requiring the support of the 2D delay-Doppler plane to be well predetermined. Clearly, the success of this algorithm depends on the size of the predetermined support set: when the support cannot be well determined, its performance is not satisfactory. However, determining such a small enough support is a difficult task because it requires the auto-ambiguity function of the transmitted signal has a good energy concentration on the 2D delay-Doppler plane: i.e., the auto-ambiguity function has a sharp main lobe and low-level side lobes.

a)Author to whom correspondence should be addressed. Electronic mail: cengwj06@mails.tsinghua.edu.cn

In this paper, a new high-resolution method is proposed for jointly estimating the multi-path time wideband delay, Doppler scale, and attenuation amplitude of a time-varying acoustic channel. The proposed method is applicable to wideband signals and does not require that the auto-ambiguity function of the transmitted signal has a good energy concentration on the 2D delay-Doppler plane.

II. PROBLEM FORMULATION

The received signal $x(t)$ of a linear time-varying channel in response to the known transmitted signal $s(t)$ is given by the superposition integral

$$x(t) = h(\tau,t) * s(t) + w(t) = \int h(\tau,t)s(t-\tau)\mathrm{d}\tau + w(t), \quad (1)$$

where * denotes linear convolution, the time-varying impulse response $h(\tau,t)$ is a function of delay time τ; and geotime t, and $w(t)$ is the additive noise and is uncorrelated with the transmitted signal. Because underwater acoustic channels are prone to multipath propagation due to reflection, scattering, and refraction, we can describe the channel impulse response $h(\tau,t)$ using a multipath model

$$h(\tau,t) = \sum_{k=1}^{K} a_k(t)\delta(\tau - \tau_k(t)), \quad (2)$$

where $\delta(\cdot)$ denotes the delta function, K is the number of paths, $a_k(t)$ and $\tau_k(t)$ are the time-varying amplitude and time delay of path k, respectively. The time variation of the delays are mainly due to the motion of the transmitter and the receiver as well as scattering of the fluctuating reflection boundaries. The path amplitudes may be also time-varying since the attenuation coefficients fluctuate with the time-variant ocean environment.

We assume the source signal $s(t)$ is transmitted as a pulse with duration T. For the duration of T, the path amplitudes are assumed time invariant, i.e., $a_k(t) = a_k$ and time variation of the delays are approximated as a Doppler scale as

$$\tau_k(t) = \tau'_k - d'_k t, \quad (3)$$

where d'_k is a constant related to relative velocity between the source and receiver of path k.

Therefore the channel impulse response can be written as

$$h(\tau,t) = \sum_{k=1}^{K} a_k \delta\big(\tau - (\tau'_k - d'_k t)\big). \quad (4)$$

Then the received signal $x(t)$ can be expressed as

$$\begin{aligned} x(t) &= \int h(\tau,t)s(t-\tau)\mathrm{d}\tau + w(t) \\ &= \sum_{k=1}^{K} a_k \int \delta\big(\tau - (\tau'_k - d'_k t)\big)s(t-\tau)\mathrm{d}\tau + w(t) \\ &= \sum_{k=1}^{K} a_k s\big(t - (\tau'_k - d'_k t)\big) + w(t) \\ &= \sum_{k=1}^{K} a_k s\big((1+d'_k)t - \tau'_k\big) + w(t). \end{aligned}$$

For the purpose of convenience, we define $\tau_k = \tau'_k/(1+d'_k)$ and $1 + d'_k = d_k$, then $x(t)$ is

$$x(t) = \sum_{k=1}^{K} a_k s(d_k(t-\tau_k)) + w(t), \quad (5)$$

which means that the received signal is the sum of K time delayed, amplitude attenuated, and Doppler scaled replicas of $s(t)$. In fact, the Doppler scale satisfies

$$d_k = 1 + \frac{v_k}{c}$$

where c is the sound speed and v_k is the radial velocity of the source relative to the receiver of the kth path. Note that v_k is positive (negative) when the source and the receiver are moving closer (far way) from each other.

In the general case, the time-varying channel estimation involves identifying $h(\tau,t)$ from the known transmitted signal $s(t)$ and the received signal $x(t)$. However, under the multipath channel model of Eqs. (4) and (5), the time-varying channel estimation problem is reduced to estimate the multipath time-delays τ_k, amplitudes a_k, and Doppler scales d_k $(k = 1,\ldots,K)$.

When the transmitted signal $s(t)$ is narrowband, i.e., it satisfies the so-called *narrowband approximation*,[5] the effect of *Doppler scale* d_k can be approximated by the *Doppler frequency shift* f_{d_k} shown as

$$f_{dk} \approx \frac{v_k}{c} f_c. \quad (6)$$

where f_c is the carrier frequency of the transmitted signal. As a result, the received signal can be expressed as

$$x(t) = \sum_{k=1}^{K} a_k s(t-\tau_k)e^{\mathrm{j}2\pi f_{d_k} t} + w(t), \quad (7)$$

i.e., the received signal is the superposition of K time delayed, amplitude attenuated, and frequency shifted replicas of $s(t)$. Denote the bandwidth and the time duration of the transmitted signal as W and T, respectively. Only when both of the following two conditions, namely,

$$W/f_c \ll 1 \quad (8)$$

and

$$WT \ll \frac{c}{2v_m} \quad (9)$$

are satisfied, the narrowband approximation holds true.[5,11] Here v_m is the maximum radial velocity of the source relative to the receiver. In other words, the narrowband assumption requires that the bandwidth is much smaller than the carrier frequency and the time-bandwidth product is much smaller than $c/2v_m$ Usually the narrowband approximation is sufficiently accurate for most wireless and radar applications but less accurate for sonar and other acoustic systems due to the low carrier frequency as well as the low sound

velocity. Several methods considered the multipath time delay and Doppler frequency shift estimation in the narrowband case.[5] However, our model in Eq. (5) is not only applicable to narrowband signals but also to wideband signals.

III. WIDEBAND CROSS-AMBIGUITY FUNCTION AND THE RAYLEIGH RESOLUTION LIMITS

The matched filtering is widely used for estimating the 2D delay-Doppler function. In the case of wideband signals, the matched filtering involves computing the wideband cross-ambiguity function (WCAF) of the transmitted signal $s(t)$ and the received signal $x(t)$, which is defined as

$$\chi_{xs}(\tau,d)=E\left[x(t)\sqrt{d}s(d(t-\tau))\right], \tag{10}$$

where $E[\cdot]$ denotes the expectation. The purpose of introducing the factor $\sqrt{d}$ is to make $s(t)$ and its Doppler-scaled version $s(d(t-\tau))$ have the same energy, namely,

$$E\left[s^2(t)\right]=E\left[\left(\sqrt{d}s(d(t-\tau))\right)^2\right]. \tag{11}$$

If there is no Doppler effect, then the Doppler scale is $d=1$ and the WCAF reduces to the cross correlation function. Substituting Eq. (5) into Eq. (10) gives

$$\chi_{xs}(\tau,d)=\sum_{k=1}^{K}a_k\chi_s\left(d_k(\tau-\tau_k),\frac{d}{d_k}\right) \tag{12}$$

where $\chi_s(\tau,\mathrm{d})$ is the wideband auto-ambiguity function (WAAF) of $s(t)$ which is defined as

$$\chi_s(\tau,d)=E\left[s(t)\sqrt{d}s(d(t-\tau))\right]. \tag{13}$$

Note that the absolute value of the WAAF attains the maximum at $(\tau,d)=(0,1)$, i.e.,

$$|\chi_s(\tau,d)|\le|\chi_s(0,1)|,\quad\forall\tau,d. \tag{14}$$

The proofs of Eqs. (12) and (14) are given by the Appendix. According to Eqs. (12) and (14), it can be easily seen that $|\chi_{xs}(\tau,d)|$ will have K local maxima (peaks) at $(\tau,d)=(\tau_k,d_k)$ $(k=1,\ldots,K)$ if the WAAF $\chi_s(\tau,d)$ has an ideal delay-Doppler distribution, i.e.,

$$\chi_s(\tau,d)=\begin{cases}\chi_s(0,1), & \text{if } \tau=0 \text{ and } d=1\\ 0, & \text{otherwise.}\end{cases} \tag{15}$$

In this case, the locations of the K peaks of $|\chi_{xs}(\tau,d)|$ can give an estimate of the true delay and Doppler, and the amplitudes of these peaks give the estimates of the corresponding attenuation factors.

It is clear that the delay-Doppler resolution of the WCAF method is dominated by the width of the main lobe of. $|\chi_s(\tau,d)|$ The width of the main lobe is the so called *Rayleigh resolution limit*. If two multipath components are spaced closer than the Rayleigh resolution limit, the two peaks will overlap, and the WCAF method can not distinguish the two closely spaced multipath components. In this sense, the WCAF method is viewed as a low-resolution method. To obtain a fine delay-Doppler resolution, the WCAF method requires that the transmitted signal should be carefully chosen such that the WAAF of the transmitted signal has a good energy concentration property on the 2D delay-Doppler plane. Generally speaking, the delay resolution is dominated by the bandwidth of the transmitted signal. The larger the bandwidth, the higher delay resolution. The Doppler resolution is dominated by the time duration of the transmitted signal. The longer the time duration, the higher Doppler resolution. Therefore using signals with large time-bandwidth products is helpful to enhance the delay-Doppler resolution. On the one hand, there are situations where it may be difficult for an emitter to generate and transmit a signal with a large bandwidth than with a small bandwidth. On the other hand, underwater environments that exhibit rapid time variation may not be suited to the use of signals with a long duration. If the time duration is too long, the propagation environment may have significantly changed. Hence it is important to develop super-resolution algorithms, which can achieve higher delay-Doppler resolution in the condition of smaller bandwidth and shorter time duration.

In the next section, we will develop a super-resolution method for joint estimation of delay and Doppler for wideband signals, which can greatly release the requirements of time duration and bandwidth.

IV. THE PROPOSED APPROACH

By observing Eq. (5), we find that the received signal $x(t)$ can be represented as a linear combination of K structural signals $\{s(d_k(t-\tau_k))\}_{k=1}^{K}$ parameterized by the unknown parameters $\{\tau_k,d_k\}$. Therefore it enlightens us to consider the channel parameter estimation as a problem of sparse representation. First let us define the discrete parameter sets of (d,τ).

$$d\in\mathcal{S}_d=\{d_{\min},d_{\min}+\Delta d,\ldots,d_{\max}\}, \tag{16}$$

$$\tau\in\mathcal{S}_\tau=\{\tau_{\min},\tau_{\min}+\Delta\tau,\ldots,\tau_{\max}\}, \tag{17}$$

where $(d_{\min},\ d_{\max})$, $(\tau_{\min},\ \tau_{\max})$, $(\Delta d,\Delta\tau)$ are the minimum, maximum possible value, and the searching precision of d and τ, respectively. There are $N_d=(d_{\max}-d_{\min})/\Delta d$ and $N_\tau=(\tau_{\max}-\tau_{\min})/\Delta\tau$ candidate values for d and τ. And there are N_dN_τ possible dictionaries in all need to be constructed in the sparse representation. Note that the time-delay is always positive. Thus we can take $\tau_{\min}=0$, which leads to

$$\mathcal{S}_\tau=\{0,\Delta\tau,\ldots,(N_\tau-1)\Delta\tau\}. \tag{18}$$

Clearly, it requires $K\ll N_dN_\tau$ to guarantee the estimation performance. In a practical underwater acoustic channel, this requirement is easy to be satisfied because the number of paths K is generally tens of order-of-magnitude, which is much smaller than N_dN_τ.

The signals are sampled with sampling period $T_s=\Delta\tau$ in the sampling interval $[0,(N-1)\Delta\tau]$. Hence we obtain the discrete signal $\boldsymbol{x}=[x(0),x(\Delta\tau),\ldots,x((N-1)\Delta\tau)]^T\in\mathbb{R}^N$. The matrix-vector form of Eq. (5) can be written as

$$\boldsymbol{x} = \boldsymbol{S}\boldsymbol{h} + \boldsymbol{w}, \tag{19}$$

where $\boldsymbol{w} = [w(0), w(\Delta\tau), \ldots, w((N-1)\Delta\tau)]^T$ is the noise vector, and the $N \times N_d N_\tau$ dictionary matrix $\boldsymbol{S}$ has the following block form

$$\boldsymbol{S} = [\boldsymbol{S}_1, \ldots, \boldsymbol{S}_{N_d}] \tag{20}$$

where each block $\boldsymbol{S}_i$ $(i = 1, \ldots, N_d)$ is the $N \times N\tau$ convolutional Toeplitz matrix associated with the ith searched Doppler scale parameter in $\mathcal{S}_d$ (denoted as d_i)

$$\boldsymbol{S}_i = \begin{bmatrix} s(d_i 0) & 0 & \cdots & 0 \\ s(d_i \Delta\tau) & s(d_i 0) & \cdots & \vdots \\ \vdots & \vdots & \ddots & \vdots \\ s(d_i(N-1)\Delta\tau) & s(d_i(N-2)\Delta\tau) & \cdots & s(d_i(N-N_\tau)\Delta\tau) \end{bmatrix}. \tag{21}$$

And $\boldsymbol{h}$ is an $N_d N_\tau$-dimensional vector and can be written as

$$\boldsymbol{h} = \left[\boldsymbol{h}_1^T, \ldots, \boldsymbol{h}_{N_d}^T\right]^T \tag{22}$$

with

$$\boldsymbol{h}_j = \left[\boldsymbol{h}_j(1), \ldots, \boldsymbol{h}_j(N_\tau)\right]^T \in \mathbb{R}^{N_\tau}, \quad j = 1, \ldots, N_d. \tag{23}$$

Columns of $\boldsymbol{S}$ are called the dictionaries in the context of sparse representation. Because the number of unknowns $N_d N_\tau$ is much larger than the number of observations N, the system in Eq. (19) is highly ill-conditioned. Fortunately, the received signal $\boldsymbol{x}$ is only the linear combination of the $K \ll N_d N_\tau$ columns from $\boldsymbol{S}$. Therefore the true solution of Eq. (19) is sparse. Now our problem has become how to obtain the sparsest solution of Eq. (19). However, finding the sparsest solution, which leads to an ℓ_0-norm minimization problem (the ℓ_0-norm is defined as counting the nonzero numbers of a vector), is an NP-hard combinatory optimization problem.

There exist two approaches to dealing with the intractable combinatory optimization problem. The first approach is the greedy pursuit algorithms such as matching pursuit (MP).[12] MP uses greedy search strategy for finding a sparse solution and the global optimum can not be guaranteed. In channel estimation, MP iteratively subtracts channel path contributions, which may result in errors if the channel paths are closely spaced. The other approach to sparse representation replaces the ℓ_0-norm by ℓ_1-norm, the performance of which is superior to the greedy pursuit algorithms. The ℓ_1-norm regularization based methods relax the NP-hard problem to a convex optimization one that can be efficiently solved in a polynomial-time complexity. One representative form of this class of methods is the ℓ_1-regularized least squares (ℓ_1-LS),[13] which adopts the following convex optimization

$$\min_{\boldsymbol{h}} \|\boldsymbol{x} - \boldsymbol{S}\boldsymbol{h}\|^2 + \lambda \|\boldsymbol{h}\|_1, \tag{24}$$

where $\|\boldsymbol{h}\|_1 = \sum_i |h(i)|$ is the ℓ_1-norm of $\boldsymbol{h}$ with $|\cdot|$ denoting the absolute value and $\lambda > 0$ is the regularization factor. Note that the ℓ_1-norm $\|\boldsymbol{h}\|_1$ is used to measure the sparsity of $\boldsymbol{h}$ and $\|\boldsymbol{x} - \boldsymbol{S}\boldsymbol{h}\|^2$ represents the residual fitting error. The regularization factor λ denotes the weighting coefficient of the penalization term. In addition to the ℓ_1-LS, one can also use the following second-order cone programming (SOCP) instead of (24)

$$\begin{aligned} &\min_{\boldsymbol{h}} \|\boldsymbol{h}\|_1 \\ &\text{s.t. } \|\boldsymbol{x} - \boldsymbol{S}\boldsymbol{h}\|^2 \le \varepsilon. \end{aligned} \tag{25}$$

The famous BP criterion[14] is based on Eq. (25). The regularization factor λ in Eq. (24) is equal to the inverse of Lagrange multiplier corresponding to the constraint. $\|\boldsymbol{x} - \boldsymbol{S}\boldsymbol{h}\|^2 \le \varepsilon$ For each λ, there exists a corresponding ε. Compared with Eq. (24), one advantage of Eq. (25) is that ε is easily determined from the noise variance, but λ is difficult to be determined. Therefore we use the BP criterion of Eq. (25) rather than the ℓ_1-LS criterion of Eq. (24) to find a sparse estimation of the multipath delay and Doppler parameters.

Standard scientific optimization programs for convex optimization, e.g., the interior-point method,[15] can be applied to solve the ℓ_1-minimization problems of Eqs. (24) and (25).

V. SIMULATION RESULTS

In the numerical simulations, the transmitted signal $s(t)$ is adopted as a widely used linear frequency modulated (LFM) signal[11] with carrier frequency f_c and pulse duration T. The LFM signal is also referred to as chirp signal, which can be expressed as

$$s(t) = \begin{cases} \cos(2\pi(f_c t + 0.5 r t^2)), & \text{if } 0 \le t \le T \\ 0, & \text{otherwise} \end{cases} \tag{26}$$

where r (in Hz/s) is the chirp rate. The instantaneous frequency of $s(t)$ at time t is $f(t) = f_c + rt$. Hence the bandwidth of $s(t)$ can be written as $W = f(T) - f(0) = rT$. In the simulations, the center frequency is fixed as $f_c = 800$ Hz. Herein, we consider the wideband signal case where the value of the bandwidth W is comparable with the carrier frequency f_c (i.e., $W/f_c \ll 1$ does not satisfy) or the time-bandwidth

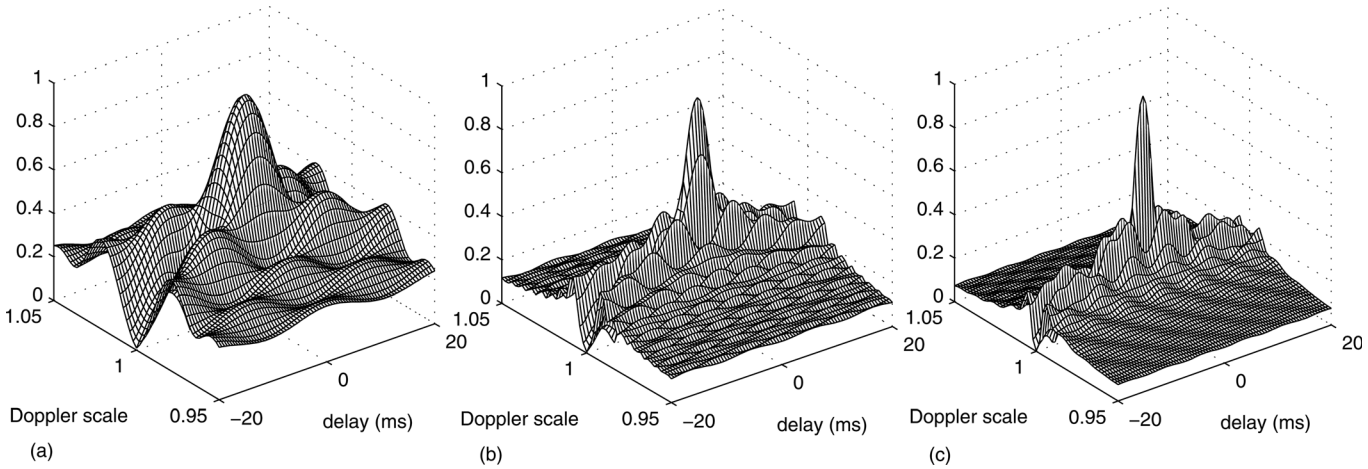

FIG. 1. Surface plots of the wideband auto-ambiguity functions (WAAF) of the LFM signals with different values of time duration T and bandwidth W. (a) $T=1$ s, $W=200$ Hz; (b) $T=2$ s, $W=400$ Hz; (c) $T=3$ s, $W=600$ Hz.

product TW has a comparable value of $c/2v_m$($TW \ll c/2v_m$ does not hold). If the maximum velocity is considered as $v_m=15$ m/s in an underwater acoustic environment, then the value of $c/2v_m$ is about 50.

As pointed out in Sec. III, the delay-Doppler resolution of the transmitted signal is related to its time duration and bandwidth. Figure 1 shows the WAAF of the LFM signals with different values of time duration and bandwidth. From Fig. 1, we can conclude that the width of the main lobe of the WAAF is dominated by the time-bandwidth product: The larger time-bandwidth product, the higher delay-Doppler resolution the WAAF has.

The signal-to-noise ratio (SNR) is defined as SNR $=10\log_{10}\left(P_s/\sigma_w^2\right)$ where P_s and σ_w^2 are the variances of the transmitted signal and the noise, respectively.

A. Simulation 1

In the first simulation, the delay-Doppler resolution capabilities of the proposed method, the WCAF, and the MP are investigated. We consider a five-component multipath channel of which the time delay (in ms), Doppler scale, and amplitude parameters are shown in Table I. Note that two pairs of the multipath components, i.e., path 1 and path 2, path 3 and path 4, are closely spaced. The delay and Doppler spaces of path 1 and path 2 (also path 3 and path 4) are set to 1 ms and 0.02.

The minimum, maximum, and the searching precision of the Doppler scale are set $d_{\min}=0.85$, $d_{\max}=1.15$, and $\Delta d=0.005$, respectively. Hence the dimension of the Doppler scale is $N_d=(d_{\max}-d_{\min})/\Delta d=60$. The sampling interval T_s and the search precision of time-delay $\Delta\tau$ are taken as $T_s=\Delta\tau;=0.5$ ms. We adopt a coarse upper bound of the maximum time-delay $\tau_{\max}=20$ ms, which leads to the dimension of delay $N_\tau=\tau_{\max}/\Delta d=40$. Hence there are $N_dN_\tau=2400$ unknown parameters to be estimated.

TABLE I. Time-delay, Doppler scale, and amplitude parameters of the multipath channel.

	Path 1	Path 2	Path 3	Path 4	Path 5
Time-delay (ms)	5	6	10	11	15
Doppler scale	0.98	1.0	1.08	1.06	0.9
Amplitude	1.0	0.99	0.98	0.97	0.95

In this simulation, the SNR is fixed as 6 dB while the time duration T and the bandwidth W are taken with a variety of values to test the delay-Doppler discriminatory capabilities of the three methods. We use two different values of T (in s) and W (in Hz): $(T,W)\in\{(0.5,200),(2,400)\}$. The corresponding time-bandwidth products are $(T,W)\in\{100,800\}$. Note that the bandwidth W has the same orders-of-magnitude as the carrier frequency f_c, which results in the violation of $W/f_c\ll 1$ In addition, the large values of time-bandwidth products used here also make the narrowband assumption of $WT\ll c/2v_m$ not satisfactory. Therefore the transmitted LFM signals are wideband.

Figure 2 shows the image plots of the multipath channel response estimates on the 2D delay-Doppler plane obtained by the WCAF, the MP, and the proposed method for the two different time-bandwidth products. To further demonstrate the estimated amplitudes of the multipath components, Fig. 3 illustrates the three-dimensional surface plots of the estimated channel responses. From Figs. 2 and 3, one can see that the resolution of the WCAF is the worst: It cannot distinguish the two closely spaced paths (path 1 and 2, path 3 and 4) when the time-bandwidth product is relative small. Moreover, the high-level side lobes of the WCAF is also disadvantageous to identify the multipath components. The MP algorithm delivers better performance than the WCAF in terms of resolution. However, it cannot correctly discriminate the two close paths at $(T,\ W)=(0.5,200)$. Some wrong peaks, which indicate incorrect multipath components, appear. Because the MP is a greedy algorithm, there is no guarantee to find the global optimal solution. Thus the performance of MP breaks down when the multipath components are closely spaced. The proposed BP based method gives accurate estimates of both time delay and Doppler scale. The proposed method breaks through the Rayleigh resolution limit, i.e., it has a super-resolution. Even in the condition of small bandwidth and short time duration, the

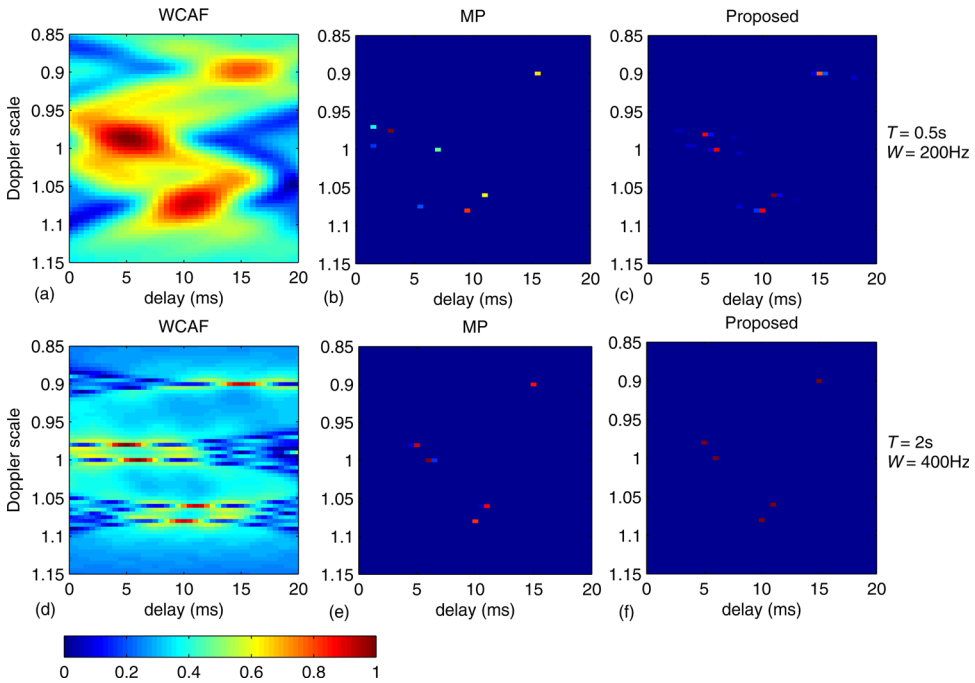

FIG. 2. (Color online) Image plots of time-delay and Doppler scale estimates with different values of time duration T (in s) and bandwidth W (in Hz) by the WCAF, the MP, and the proposed method. The 1st and 2nd rows show the results of $(T,\ W) = (0.5,\ 200)$ and (2,400), respectively.

proposed method can correctly distinguish the closely spaced multipath components.

B. Simulation 2

In the second simulation, the resolution capabilities of the three methods are further studied. Two closely spaced multipath components with equal unit amplitudes are considered. The parameters of delay (in ms) and Doppler scale of the two paths are set as $(\tau_1, d_1) = (5,1.0)$ and $(\tau_2, d_2) = (6,1.01)$. The SNR is set to 3 dB. We aim at computing the probability of success versus different time-bandwidth products through Monte Carlo trials. At each value of time-bandwidth product, 1000 Monte Carlo trials are performed. A trial is successful if it succeeds in correctly distinguishing the positions of the two paths on the 2D delay-Doppler plane. Clearly, the probability of success can indicate the resolving power of an algorithm. The time-bandwidth product TW of the LFM signal varies from 230 to 330. Note the values of the ith $(i = 0,\ldots, L-1)$ with L the number of considered time-bandwidth products, time duration, and bandwidth as T_i and W_t, respectively. The initial values are $T_0 = 1$ s, $W_0 = 230$ Hz. The relation between (T_i, W_i) and (T_0, W_0) is $T_i = \alpha_i T_0$, $W_i = \alpha_i W_0$ with $\alpha_i \geq 1$ the increasing factor. Namely, the values of T and W are increased by the same factor α_i.

Figure 4 shows the probability of success versus time-bandwidth product (from 230 to 330) of the three methods. As we can see, the probability of success of the proposed method is the highest. The proposed method and MP surmount the Rayleigh resolution limit. Thus both of them possess the capability of super-resolution. The resolution

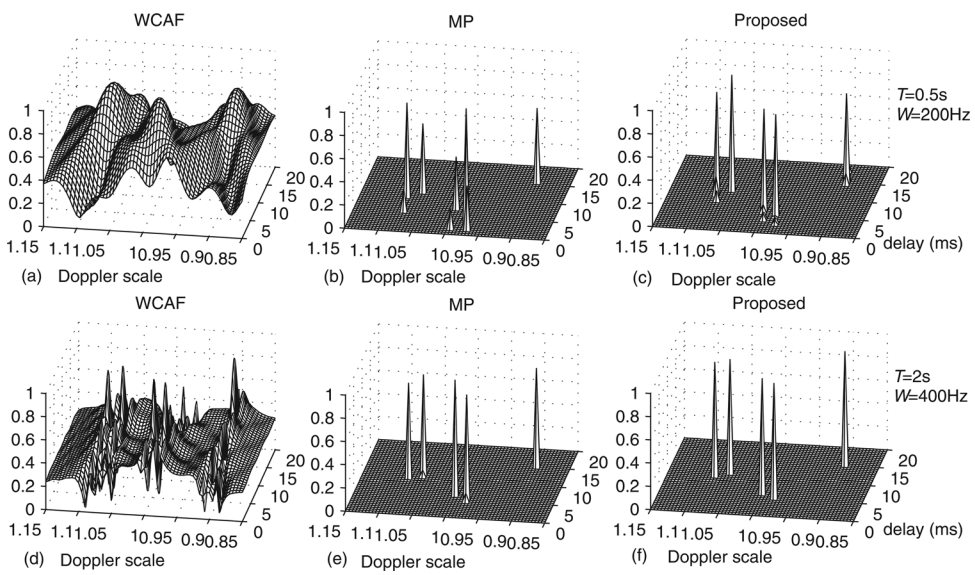

FIG. 3. Surface plots of time-delay and Doppler scale estimates with different values of time duration T (in s) and bandwidth W (in Hz) by the WCAF, the MP, and the proposed method. The 1st and 2nd rows show the results of $(T,\ W) = (0.5,200)$ and (2,400), respectively.

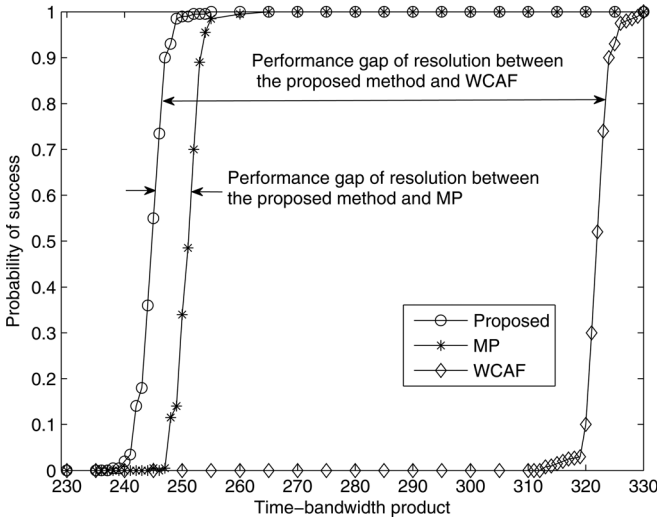

FIG. 4. Probability of success versus time-bandwidth product.

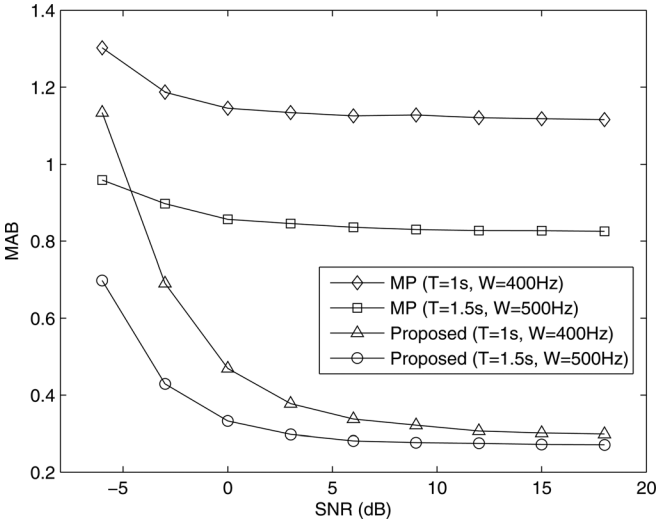

FIG. 6. Mean absolute bias (MAB) of the time-delay and Doppler scale estimates versus SNR.

performance of the WCAF has a large gap compared with our approach and the MP. Moreover, the proposed method is superior to the MP.

C. Simulation 3

In the third simulation, Monte Carlo trials are carried out to evaluate the statistical estimation performances of the MP algorithm and the proposed approach at different SNRs. We use two statistical performance indices: the mean squared error (MSE) and the mean absolute bias (MAB) of the estimated channel response, which are expressed as

$$\mathrm{MSE} = \frac{1}{M_c}\sum_{m=1}^{M_c} \left\|\hat{\boldsymbol{h}}_m - \boldsymbol{h}\right\|^2$$

and

$$\mathrm{MAB} = \frac{1}{M_c}\sum_{m=1}^{M_c} \left\|\hat{\boldsymbol{h}}_m - \boldsymbol{h}\right\|_1 = \frac{1}{M_c}\sum_{m=1}^{M_c}\sum_{i=1}^{N_d N_\tau} \left|\hat{\boldsymbol{h}}_m(i) - \boldsymbol{h}(i)\right|$$

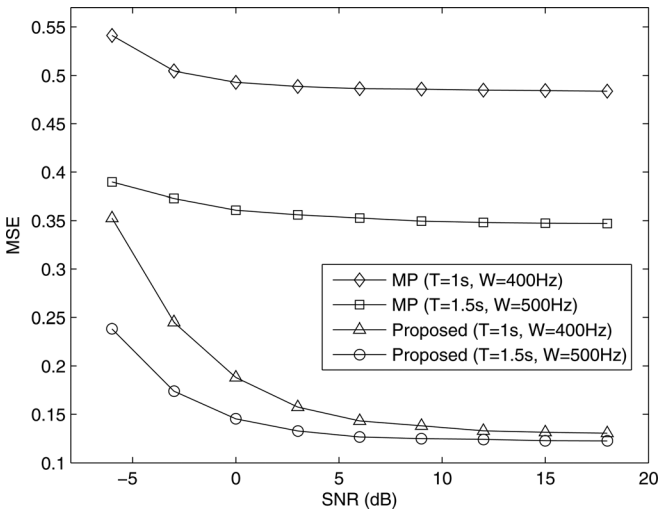

FIG. 5. Mean squared error (MSE) of the time-delay and Doppler scale estimates versus SNR.

where M_c is the number of Monte Carlo trials and $\hat{\boldsymbol{h}}_m$ is the estimated result of the mth trial. Because $\left\|\hat{\boldsymbol{h}}_m - \boldsymbol{h}\right\|_1$ is the ℓ_1-norm of the error vector, $\hat{\boldsymbol{h}}_m - \boldsymbol{h}$ the MAB is an appropriate performance index when the channel response is sparse. Note that the estimate error of the WCAF is too large; this is caused by the high-level side lobes of the ambiguity function. Therefore we do not compare the WCAF method in this simulation.

The multipath channel is the same as the one used in Simulation 1 the parameters of which are shown in Table I. We adopt two different values of time duration T (in s) and bandwidth W (in Hz). One is $(T, W) = (1,400)$, the other is $(T, W) = (1.5, 500)$. At each value of (T, W), the SNR varies from -6 dB to 18 dB. For each SNR, $M_c = 1000$ Monte Carlo trials are performed.

Figures 5 and 6 illustrate the MSE and MAB of the estimated channel response versus SNR, respectively. Clearly, the estimates by the proposed method are much more accurate than those obtained by the MP algorithm.

VI. CONCLUSION

We formulate the problem of estimating the multipath time delay, amplitude, and Doppler scale parameters of a time-varying acoustic channel as a problem of sparse representation. The ℓ_1-norm regularization technique is adopted to reduce the ill-conditioning, which leads to a tractable convex optimization problem. The proposed method is applicable to wideband signals and does not require any constraints on the property of the auto-ambiguity function of the transmitted signal. Simulation results illustrate that the proposed method has a super-resolution on the 2D delay-Doppler plane.

ACKNOWLEDGMENT

The authors would like to thank the anonymous reviewers for their insightful, helpful and constructive advices that greatly improved the quality of this manuscript. This work was supported by the Chinese 863 high-tech program under Grant 2009AA12Z308 and the National Natural Science Foundation of China under Grant No. 61071150.

APPENDIX: DERIVATIONS

In this appendix, we will prove Eqs. (12) and (14). By the definition of WCAF and using Eq. (5), we have

$$\chi_{xs}(\tau,d) = E\left[x(t)\sqrt{d}s\ (d(t-\tau))\right] = \sum_{k=1}^{K} a_k E\left[s(d_k(t-\tau_k))\sqrt{d}s(d(t-\tau))\right] + \chi_{ws}(\tau,d), \tag{A1}$$

where $\chi_{ws}(\tau,d) = E[w(t)s(d(t-\tau))]$ is the WCAF of $w(t)$ and $s(t)$. Because the noise $w(t)$ is uncorrelated with the transmitted signal $s(t)$, the term of $\chi_{ws}(\tau, d)$ will vanish. Letting, $d_k(t-\tau_k) = u$, i.e., $t = \frac{u}{d_k} + \tau_k$, then we obtain

$$\begin{aligned} &E\left[s(d_k(t-\tau_k))\sqrt{d}s\ (d(t-\tau))\right] \\ &= E\left[s(u)\sqrt{d}s\left(d\left(\frac{u}{d_k}+\tau_k-\tau\right)\right)\right] \\ &= E\left[s(u)\sqrt{d}s\left(\frac{d}{d_k}(u-d_k(\tau-\tau_k))\right)\right] \\ &= \chi_s\left(d_k(\tau-\tau_k), \frac{d}{d_k}\right). \end{aligned} \tag{A2}$$

Plugging Eq. (A2) into Eq. (A1) immediately gives Eq. (12).

By the Cauchy–Schwartz inequality, it follows

$$\begin{aligned} |\chi_s(\tau,d)|^2 &= E^2\left[s(t)\sqrt{d}s(d(t-\tau))\right] \\ &\le E\left[s^2(t)\right]E\left[\left(\sqrt{d}s(d(t-\tau))\right)^2\right] \\ &= |\chi_s(0,1)|^2, \end{aligned} \tag{A3}$$

where we have used the fact that

$$E\left[\left(\sqrt{d}s(d(t-\tau))\right)^2\right] = E\left[s^2(t)\right] = \chi_s(0,1).$$

Equation (A3) immediately concludes Eq. (14).

[1] P. L. Ainsleigh, "Acoustic echo detection and arrival-time estimation using spectral tail energy," J. Acoust. Soc. Am. **110**, 967–972 (2001).
[2] E. K. Westwood and D. P. Knobles, "Source track localization via multipath correlation matching," J. Acoust. Soc. Am. **102**, 2645–2654 (1997).
[3] N. F. Josso, C. Ioana, and J. Mars, "On the consideration of motion effects in the computation of impulse response for underwater acoustics inversion," J. Acoust. Soc. Am. **126**, 1739–1751 (2009).
[4] W.-J. Zeng, X. Jiang, X.-L. Li, and X.-D. Zhang, "Deconvolution of sparse underwater acoustic multipath channel with a large time-delay spread," J. Acoust. Soc. Am. **127**, 909–919 (2010).
[5] M. D. Hahm, Z. I. Mitrovski, and E. L. Titlebaum, "Deconvolution in the presence of Doppler with application to specular multipath parameter estimation," IEEE Trans. Signal Process. **45**, 2203–2219 (1997).
[6] A. W. Habboosh, R. J. Vaccaro, and S. Kay, "An algorithm for detecting closely spaced delay/Doppler components," in *Proceedings of the ICASSP* (1997), pp. 535–538.
[7] D. J. Nelson and D. C. Smith, "Scale cross-ambiguity and target resolution," Digit. Signal Process. **19**, 194–200 (2009).
[8] C. H. Knapp and G. C. Carter, "Estimation of time delay in the presence of source or receiver motion," J. Acoust. Soc. Am. **61**, 1545–1549 (1977).
[9] R. J. Vaccaro, C. S. Ramalingam, D. W. Tufts, and R. L. Field, "Least squares time-delay estimation for transient signals in a multipath environment," J. Acoust. Soc. Am. **92**, 210–218 (1992).
[10] Z.-H. Michalopoulou and M. Picarelli, "Gibbs sampling for time-delay and amplitude estimation in underwater acoustics," J. Acoust. Soc. Am. **117**, 799–808 (2005).
[11] J. P. Hermand and W. I. Roderick, "Delay-Doppler resolution performance of large time-bandwidth-product linear fm signals in a multipath ocean environment," J. Acoust. Soc. Am. **84**, 1709–1727 (1988).
[12] S. Mallat and Z. Zhang, "Matching pursuits with time-frequency dictionaries," IEEE Trans. Signal Process. **41**, 3397–3415 (1993).
[13] S.-J. Kim, K. Koh, M. Lustig, S. Boyd, and D. Gorinevsky, "An interior-point method for large-scale ℓ_1-regularized least squares," IEEE J. Sel. Top. Signal Process. **1**, 606–617 (2007).
[14] S. Chen, D. L. Donoho, and M. A. Saunders, "Atomic decomposition by basis pursuit," SIAM Rev. **43**, 129–159 (2001).
[15] S. Boyd and L. Vandenberghe, *Convex Optimization* (Cambridge University Press, Cambridge, 2006), Chap. 11, pp. 561–615.